JKAU: Eng. Sci., Vol. **32** No. 2, pp: 89 – 100 (1444 A.H. / 2022 A.D.)
Doi: 10.4197/Eng. 32-2.7

Effects of Piston motion on the power generated by Stirling cycle machines

Majed M. Alhazmy*

Mechanical Engineering, King Abdulaziz University, Jeddah, Saudi Arabia

Abstract. This paper uses a simple model to estimate the power output of Stirling engine when giving the pistons a continuous motion with a prescribed pattern, fixed frequency, and a variable phase shift for different operational temperature ratios. Two continuous motions patterns, sinusoidal and modified sinusoidal, have been examined against the discontinuous motion of the ideal cycle. The power produced from engines having continuously moving pistons is lower than the power produced from the ideal cycle. The power ratio decreases as the temperature ratio increases. the highest produced power with a temperature ratio of 1.5, is 97% of the ideal cycle and it occurs at a phase-shift of 81°. Operating at ±10° off the highest power phase shift condition reduces the output power by 5-7%. For modified sinusoidal motion, the highest output power is 88% when the phase shift is 55°. Operating at ±10° off the maximum power phase shift condition reduces the output power by 2%. Moreover, at the highest output phase shift condition, the power output ratio drops from 97% to 93%, for sinusoidal motion as the cycle temperature ratio changes from 1.5 to 3. For modified sinusoidal motion, the output power drops from 88% to 78% at the highest phase shift condition.

Keywords. Stirling machines, Piston's discontinuous motion, Piston's continuous motion Performance of Stirling machines

1. Introduction

Oil high prices, pollution control, and global warming reducing policies call for replacing the traditional power systems with environmentally safe power sources [1-3]. Stirling cycle machines operated by solar energy or waste heat are promising future solutions for engines [4] and coolers [5]. Stirling machines are regenerative closed cycle machines that have low noise levels and high efficiency and can operate at low temperatures or at elevated temperatures [6].

Figure 1 shows an ideal Stirling cycle that consists of four reversible processes performed by inviscid ideal working fluid. The four processes of the Stirling cycle are isochoric heat addition, isothermal expansion, isochoric heat rejection and isothermal compression. Figure 2 shows a schematic of the Stirling machine. The machine has two pistons each is contained inside a separate isothermal cylinder. The piston-cylinder arrangement is called working space that is maintained at a specific temperature. The two cylinders are connected by an ideal regenerator. The working fluid shuttles

* Corresponding author: mhazmy@kau.edu.sa

between the two working spaces absorbs and rejects heat as it moves between the two working spaces.

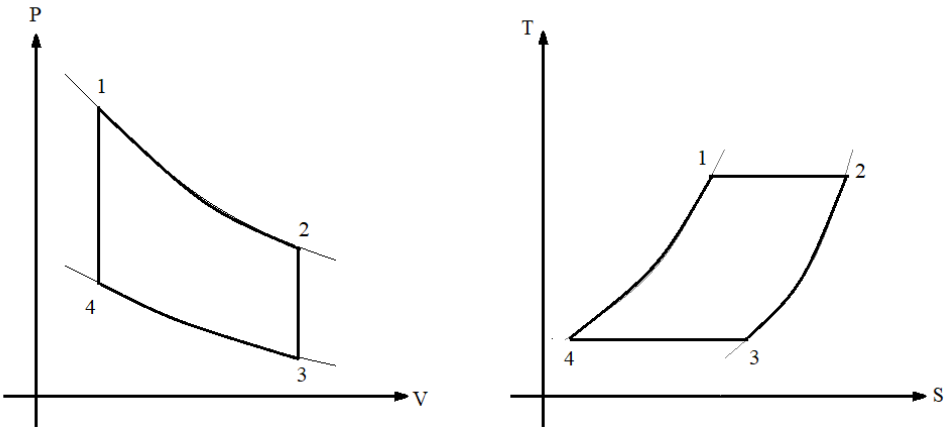

(a) (b)

Figure 1 Stirling Cycle, (a) PV diagram, (b) TS diagram

Efforts to improve the performance of Stirling machines never stop, several attempts have been reported in the literature [7-11]. These include optimizing operating temperature and pressure ratios [7-8], comparing different working fluids [9], examining the effect of the ratio of the dead volume and the details of the piston motion [10-12]. Results of both experimental and analytical studies on the performance of Stirling engines [13], Stirling heat pumps [14-15], and Stirling liquefiers and coolers [16-18] are available.

The pistons of the ideal Stirling cycle have a discontinues motion, the pistons in real Stirling machines, however, move in continuous motion. Discontinues motion is difficult to maintain, therefore, sinusoidal motion is usually the chosen pattern. Although Sinusoidal motion is easy to maintain, it yields a lower performance compared to discontinuous motion. This is expected because the pistons speed in sinusoidal motion is slower near the cylinder's two dead centers and faster near the middle of the stroke. This does not happen in the discontinuous motion. The difference in the motion pattern determines the change in the mass flow rate of the working fluid entering to and leaving (or dwelling) the working spaces the ultimately affects the performance of the machine because. The details the motion of the pistons along with the type of the thermal process determine the changes in temperature and pressures of the working fluid throughout the different states of the cycle, and therefore, the shape of the thermodynamic cycle.

Ranieri et al [19] reported a 65% reduction in the efficiency when the pistons of an alpha type Stirling engine have a sinusoidal motion. Červenka [20] reported a power drop by 82% when pistons move in sinusoidal motion compared to the discontinuous motion of the ideal cycle. Briggs [21] achieved 14% power increase by manipulated electrically the sinusoidal volume change of a free-piston Stirling engine. By using a linear electric motor Gopal [22] reported a 15% increase in efficiency. Craun and Bemiah [23] reported that a non-sinusoidal motion enhances the performance of the Stirling engine by 40% more than to sinusoidal motion. Masser et al [24] reported that the

cycle output power may increase when the pistons motion adjusted to a modified type of a sinusoidal motions. An optimum performance should balance between maximizing the output power and the overall performance [24-25]. A way to minimize the deviation between the sinusoidal and the discontinuous motion to control the phase shift between the motion of the compression piston and the expansion piston [26-28].

The aim of the present paper is to show the effect of the motion pattern on the performance of a Stirling engine. The heat addition and heat rejection in Stirling cycle occur along isothermal processes, therefore, the power output is chosen to be the performance indicator to compare effect of different motion patterns. The two pistons are given are prescribed motion with a fixed frequency and a phase shift. Two different motion patterns, sinusoidal and modified sinusoidal, are examined against the discontinuous motion of the ideal cycle, at different operational temperature ratios and different angles of phase shifts.

2. Analysis

Figure 2 shows a schematic of a Stirling engine that consists of an expansion space, a hot heat exchanger, a regenerator, a cold heat exchanger, and a compression space. The expansion and compression spaces are called working spaces. Each working space is a piston moving inside a cylindrical chamber and encloses ideal gas as the working fluid. As the pistons move the fluid transfers from one expansion spaces through the two heat exchangers and the regenerator until it reaches the other working space.

In details, as pistons move, the volume and the pressure in each compartment of the machine change. The pressure difference causes the mass to move from one side of the machine to the other. Urieli and Berchowitz [6] presented a simple model for these changes, based on which a theoretical model to relate the machine performance is presented below. The analysis assumes that the working is ideal gas, perfect regenerator, isothermal heat exchangers, and adiabatic hot and the cold working spaces.

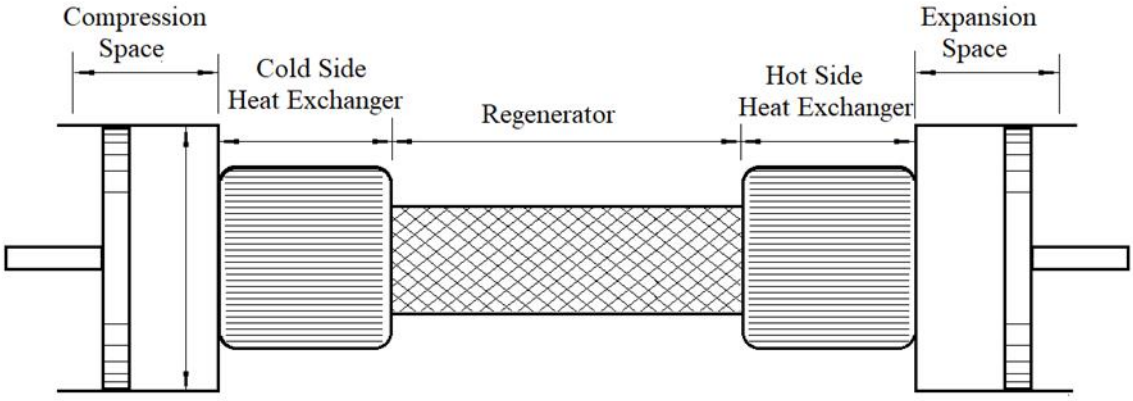

Figure 2. Schematic of a typical Stirling Engine

The model starts by describing the motion, x_c and x_e of the compression and expansion pistons, respectively, as a function of time. There is a time lag (phase shift), α, between the motion of the two pistons, Eq. (1).

$$\left.\begin{aligned} x_c(t) &= f_c(t) \\ x_e(t) &= f_e(t+\alpha) \end{aligned}\right\} \quad (1)$$

The volume of each working space depends on the piston position as,

$$\left.\begin{aligned} V_c(t) &= A_c\, x_c(t) + V_{dc} \\ V_e(t) &= A_e\, x_e(t) + V_{de} \end{aligned}\right\} \quad (2)$$

Note that A_c and A_e are the cross-sectional areas of the compression and expansion spaces, respectively, similarly, V_{dc} and V_{de} are the dead volumes in the compression and expansion spaces, respectively. Although the mass of the working fluid in each compartment changes during operation, the total mass filling up all the compartments of the Engine is constant,

$$M_{tot} = m_c + m_k + m_r + m_h + m_e \quad (3)$$

But dM_{tot}=0 Therefore,

$$dm_c + dm_k + dm_r + dm_h + dm_e = 0 \quad (4)$$

The ideal gas law relates the mass of the fluid occupying each compartment of the engine to the volume, pressure and temperature of each compartment as follows,

$$\left.\begin{aligned} m_c &= \frac{P\,V_c}{R\,T_c} \\ m_k &= \frac{P\,V_k}{R\,T_k} \\ m_r &= \frac{P\,V_r}{R\,(T_e - T_c)\,ln\left(\frac{T_e}{T_c}\right)} \\ m_h &= \frac{P\,V_h}{R\,T_h} \\ m_e &= \frac{P\,V_e}{R\,T_e} \end{aligned}\right\} \quad (5)$$

Substituting the relations from Eq. (5) into Eq. (3) yields,

$$M_{tot} = \frac{P\,V_c}{R\,T_c} + \frac{P\,V_k}{R\,T_k} + \frac{P\,V_r}{R\,(T_e - T_c)\,ln\left(\frac{T_e}{T_c}\right)} + \frac{P\,V_h}{R\,T_h} + \frac{P\,V_e}{R\,T_e} \quad (6)$$

To obtain the mass flow rate entering or leaving each compartment, one may use the first law of thermodynamics in the differential form. In the absence of the variations in kinetic and potential energy, and assuming the working fluid to be an ideal gas the first law of thermodynamics in the differential form is

$$dE_{cv} = \delta Q - \delta W + dH_{in} - dH_{out} \quad (7)$$

The heat exchangers, the regenerator, and each working space, at every instant, either receive or deliver fluid, moreover, the compression space is adiabatic, and the work is a boundary work $W = P\,dV$, therefore the first law of thermodynamics, Eq. (7), becomes,

$$c_v\ d(m_c T_c) = -P\,dV_c + c_p\,T_c\,dm_c \quad (8)$$

Note that for ideal gas $m\,T = \frac{P\,V}{R}$, therefor Eq (8) can be rewritten as

$$\frac{c_v}{R}\,[P\,dV_c + V_c\,dP] = -P\,dV_c + c_p\,T_c\,dm_c \quad (9)$$

Rearranging Eq. (9), the change in the mass inside the compression space becomes

$$dm_c = \frac{\frac{V_c}{\gamma}dP + P\,dV_c}{RT_c} \quad (10)$$

Similarly, the change in the mass in the expansion space is,

$$dm_e = \frac{\frac{V_e}{\gamma}dP + P\,dV_e}{RT_e} \quad (11)$$

The volume and the temperature of each heat exchanger and the regenerator are fixed, therefore the ideal gas law gives the change in the mass inside them as

$$\left.\begin{aligned} dm_k &= \frac{V_k}{RT_k}dP \\ dm_r &= \frac{V_r}{RT_r}dP \\ dm_h &= \frac{V_h}{RT_h}dP \end{aligned}\right\} \quad (12)$$

The mass balance on the heat exchangers gives,

$$\left.\begin{aligned} m_{ck} &= -dm_c \\ m_{kr} &= m_{ck} - dm_c \\ m_{eh} &= dm_e \\ m_{rh} &= m_{he} - dm_h \end{aligned}\right\} \quad (13)$$

Substituting from Eqs. (10)-(13) into Eq.(4), the change in the pressure in the machine is,

$$dP = \frac{-\gamma P\left(\frac{dV_c}{T_c}+\frac{dV_e}{T_e}\right)}{\frac{V_c}{T_c}+\gamma\left(\frac{V_{hc}}{T_{hc}}+\frac{V_r}{T_r}+\frac{V_e}{T_e}\right)+\frac{V_e}{T_e}} \quad (14)$$

The change in the temperature of the fluid inside the compression and expansion spaces can be related to the change in the mass, volume, and pressure through the ideal gas law as

$$\left.\begin{aligned} dT_c &= T_c\left(\frac{dP}{P}+\frac{dV_c}{V_c}-\frac{dm_c}{m_c}\right)\\ dT_e &= T_e\left(\frac{dP}{P}+\frac{dV_e}{V_e}-\frac{dm_e}{m_e}\right)\end{aligned}\right\} \quad (15)$$

The above analysis shows how the properties of the working fluid are related and calculated once the motion of each piston is known. The expansion and compression work can then be evaluated as

$$\left.\begin{aligned} dW_c &= PdV_c\\ dW_e &= PdV_e\\ dw &= dW_c + dW_e\end{aligned}\right\} \quad (16)$$

$$W = W_c + W_e \quad (17)$$

Results and discussions

The model presented above yields the power output from Stirling engine when the motion of the pistons is defined. The model power output is evaluated for three different motion patterns given by Eqs. (18)-(23). Equations (18) and (19) show the first pattern, it is the discontinues motion of the ideal Stirling cycle. This motion is plotted in a dimensionless scale in Fig 3 (a) for the compression piston, x_{1c}, and the expansion piston x_{1e}.

$$x_{1c} = \begin{cases} 1 & 0 \le t \le \frac{\pi}{2\omega}\\ 2-2\frac{\omega t}{\pi} & \frac{\pi}{2\omega} \le t \le \frac{\pi}{\omega}\\ 0 & \frac{\pi}{\omega} \le t \le \frac{3\pi}{2\omega}\\ 2\frac{\omega t}{\pi}-3 & \frac{3\pi}{2\omega} \le t \le \frac{\pi}{\omega}\end{cases} \quad (18)$$

$$x_{1e} = \begin{cases} \frac{2\omega}{\pi}t & 0 \le t \le \frac{\pi}{2\omega}\\ 1 & \frac{\pi}{2\omega} \le t \le \frac{\pi}{\omega}\\ 3-2\frac{\omega t}{\pi} & \frac{\pi}{\omega} \le t \le \frac{3\pi}{2\omega}\\ 0 & \frac{3\pi}{2\omega} \le t \le \frac{\pi}{\omega}\end{cases} \quad (19)$$

Similarly, equations (20) and (21) show the second motion pattern, it is a typical continuous sinusoidal motion as plotted in a dimensionless scale in Fig 3 (b) with a phase shift, α, between the compression piston, x_{2c}, and the expansion piston x_{2e}.

$$x_{2c} = 1 + \cos(\omega t) \quad (20)$$

$$x_{2e} = 1 + \cos(\omega t + \alpha) \quad (21)$$

Similarly, equations (22) and (23) show the third motion pattern, it is a modified sinusoidal motion. It consists of two sin functions combined by two constants B_1 and B_2 as plotted in a dimensionless scale in Fig 3 (c) with a phase shift, α, between the compression piston, x_{3c}, and the expansion piston x_{3e}.

$$x_{3c} = \frac{B_1\cos(\omega t)+\sqrt{\left(B_2^2-B_1^2\sin^2(\omega t)\right)}}{B_1+B_2} \quad (22)$$

$$x_{3e} = \frac{B_1\cos(\omega t+\alpha)+\sqrt{\left(B_2^2-B_1^2\sin^2(\omega t+\alpha)\right)}}{B_1+B_2} \quad (23)$$

where B_1 and B_2 are constant parameters to define the piston's motion profile and the dwelling duration (angle) [25].

Figure 3 shows the position of the pistons during a full working cycle for discontinuous ideal pattern as well as for the two continuous motions with a specified phase shift between the compression and expansion pistons. Similarly, Fig. 4 shows the Stirling cycle resulted from such motions, plotted on the P-V diagram, at the highest work output condition.

Figure 5 shows the power output for the sinusoidal motion, Eqs. (20)-(21) and Fig. 3 (b), as a ratio to the power produced by an ideal cycle operating at the same temperature ratio, t. The results show that low temperature ratios bring the output power closer to the output of ideal cycle for all phase shift angles. The highest output power reached is 97% of the ideal cycle, it occurs at a phase shift, α, of 81°. Moreover, the output power changes with the phase shift. Operating at ±10° of the maximum power phase shift condition reduces the output power by 5-7%.

(a)

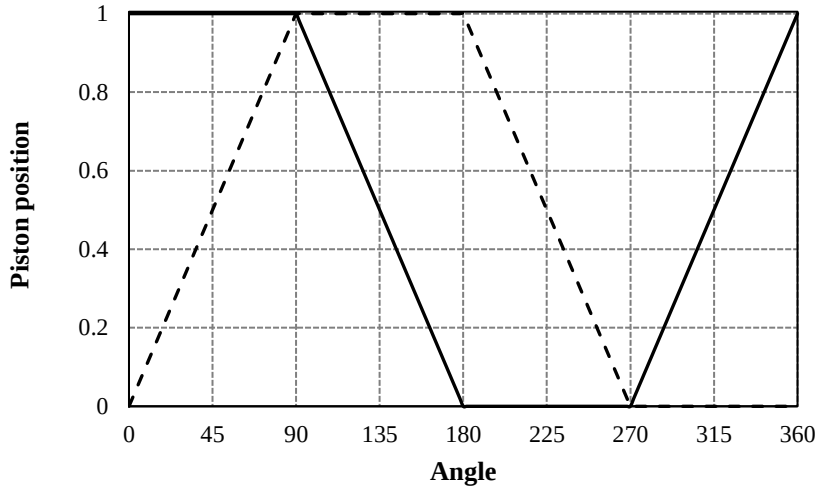

(b)

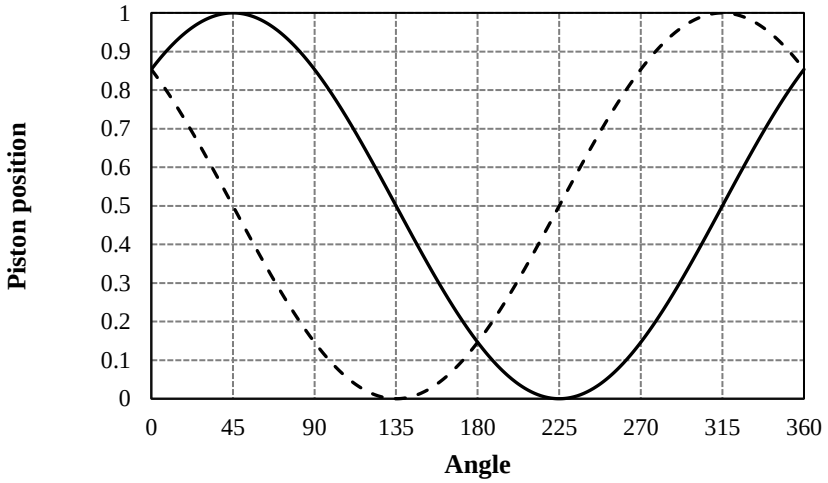

(c)

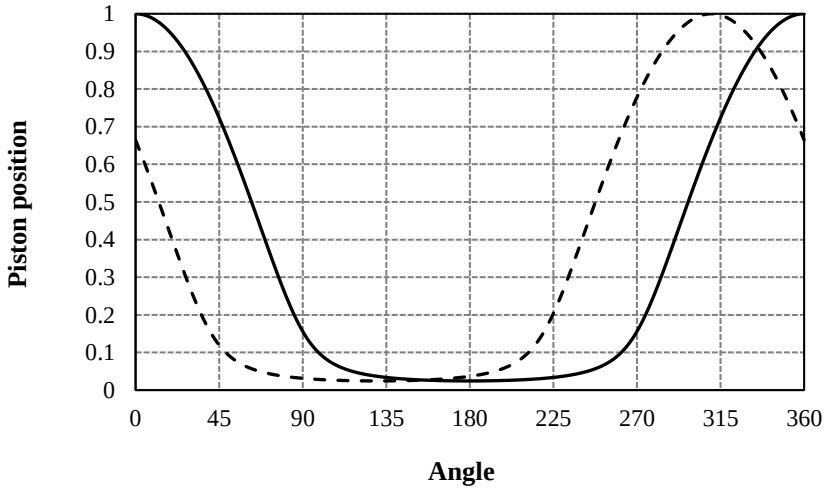

Figure 3. The three examined piston's motions
(__ compression, _ _ _ compression)

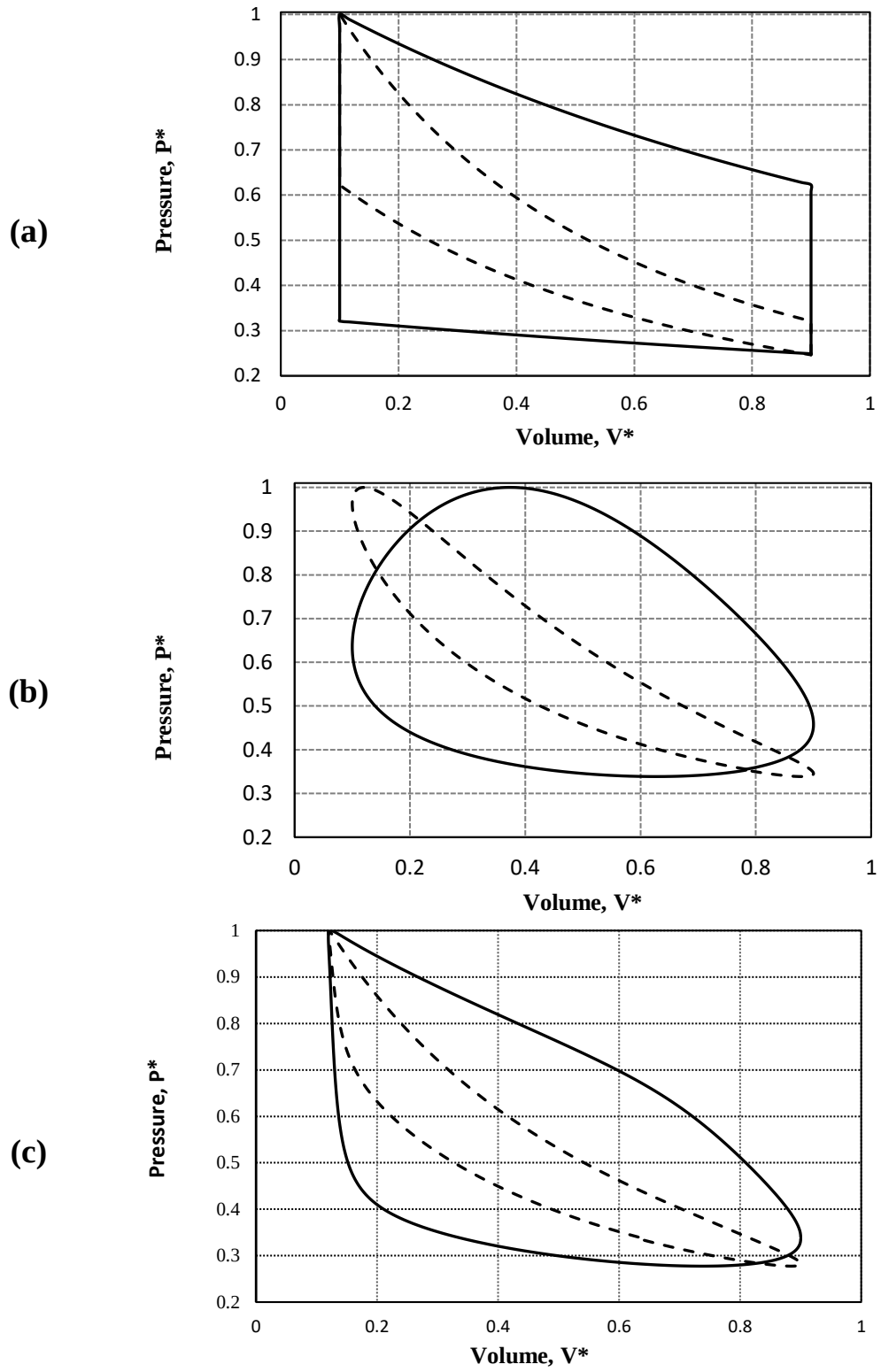

Figure 4. The Stirling cycle as P V plot fir the three piston's motions
(__ compression, _ _ _ compression)

Similarly, Fig. 6 shows the power output ratio when the piston has the modified motion given by Eqs. (22)-(23) and Fig. 3 (c). The highest output power reached is 88% of the power from an ideal cycle and obtained a phase shift of 55º.

Operating at ±10° of the maximum power phase shift condition reduces the output power by 2%.

Moreover, at the highest output phase shift condition, the power output ratio drops from 97% to 93%, as the cycle temperature ratio changes from 1.5 to 3, for sinusoidal motion pattern. For modified sinusoidal motion, the output power drops from 88% to 78% at the highest phase shift condition

.

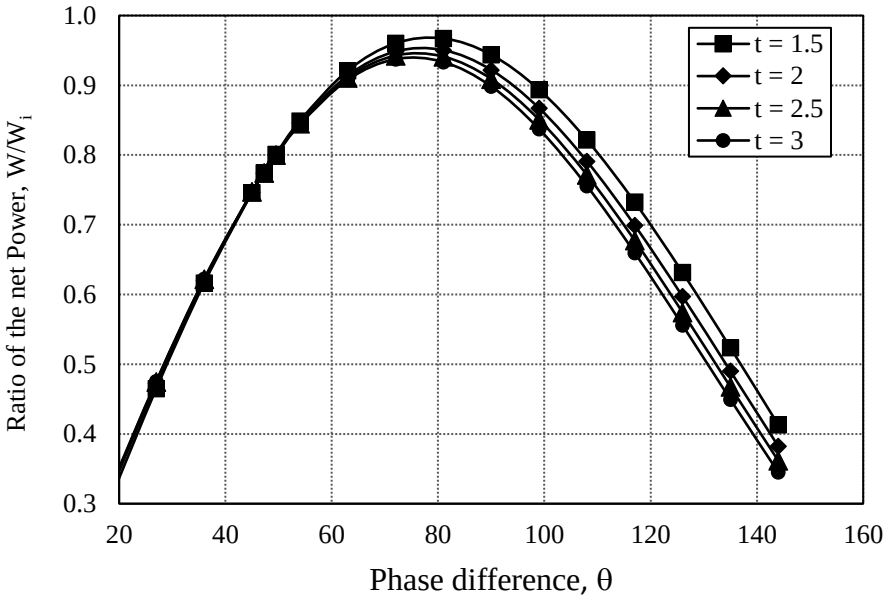

Figure 5. Variation of output power with phase shift for different temperature ratios (Sinusoidal motion).

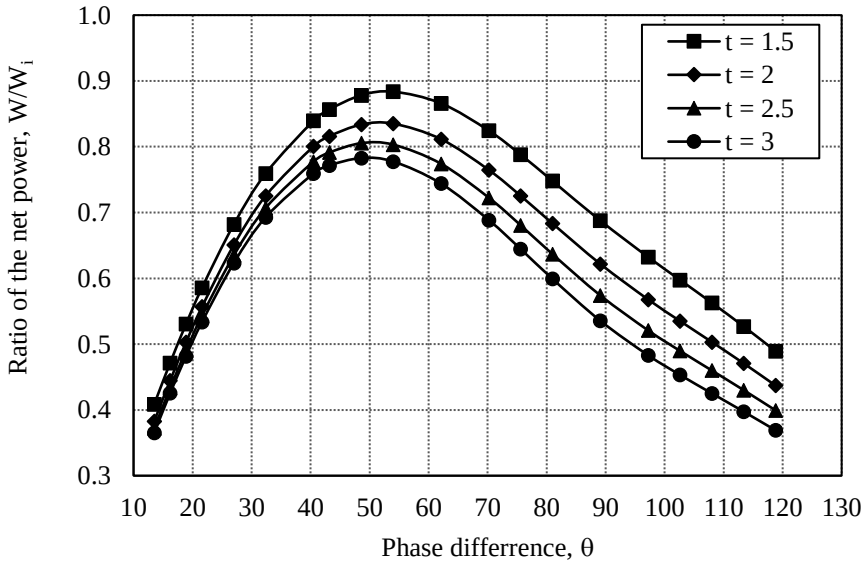

Figure 6. Variation of output power with phase shift for different temperature ratios (Modified motion).

Conclusions

The piston motion effect on the power output from a Stirling cycle machine is evaluated. The power produced when the pistons have continuous motion is lower than the power produced from the ideal cycle for all operational temperature ratios. The power ratio decreases as the temperature ratio increases. For a temperature ratio of 1.5, the highest produced power is 97% of the ideal cycle and occurs that occurs and phase-shift of 81^o. Operating at ±10^o off the highest power phase shift condition reduces the output power by 5-7%. For modified sinusoidal motion, the highest output power is 88% when the phase shift is 55^o. Operating at ±10^o off the maximum power phase shift condition reduces the output power by 2%. Moreover, at the highest output phase shift condition, the power output ratio drops from 97% to 93%, for sinusoidal motion as the cycle temperature ratio changes from 1.5 to 3. For modified sinusoidal motion, the output power drops from 88% to 78% at the highest phase shift condition.

Nomenclature

A	Cross sectional Area of the working space
B_1&B_2	Parameters describing the modified motion pattern Eq.(22)-(23)
c_p	Fluid specific heat at constant pressure
c_v	Fluid specific heat at constant volume
M	Total mass of the working fluid filling the machine
m	Mass of the working fluid inside each compartment of the machine
P	Pressure
Q	Heat
R	Gas constant
S	Entropy
T	Temperature
V	Volume
x	Position of the pistons
W	Work

Symbol

α	Phase shift
γ	Specific heat ratio
ω	Frequency

Subscripts

c	Compression space
e	Expansion space
dc	Dead volume compression side
de	Dead volume expansion side
in	Inlet
out	Outlet
h	Heat exchanger at hot side
k	Heat exchanger at cold side

References

[1] **She X., Cong L., and Nie B.**, Energy-efficient and-economic technologies for air conditioning with vapor compression refrigeration: a comprehensive review. Applied Energy, 232:157–86 (2018).

[2] **Abas N., Kalair A.R., and Khan N.**, Natural and synthetic refrigerants, global warming: a review. Renewable and Sustainable Energy Reviews, 90:557–69 (2018).

[3] Sadovskaia K, Bogdanov D, Honkapuro S, and Breyer, C. Power transmission and distribution losses–A model based on available empirical data and future trends for all countries globally. International Journal of Electrical Power and Energy Systems. 107:98–109 (2019).

[4] **He M.M.** Stirling engine for solar thermal electric generation.

University of California; Berkeley, (2016).

[5] **Lu, D., Bai, Y., Zhao, Y., Dong, X., Gong, M., Luo, E., Chen, G., Xu, Q. and Shen, J.**, Experimental investigations of an absorption heat pump prototype with intermediate process for residential district heating. Energy Conversion and Management, 204, p. 112323 (2020).

[6] **Urieli I., and Berchowitz D.M.,** Stirling cycle engine analysis, A. Hilger, (1984).

[7] **Hu JY, Luo EC, Dai W, and Zhang LM.** Parameter sensitivity analysis of duplex Stirling coolers. Applied Energy.190:1039-46 (2017).

[8] **Pan QW, and Wang RZ.** Study on boundary conditions of adsorption heat pump systems using different working pairs for heating application. Energy Conversion and Management, 154:322–35 (2017).

[9] **Doğan B., Ozturk M.M., and Erbay L.B.,** Effect of working fluid on the performance of the duplex Stirling refrigerator. Journal of Cleaner Production,189:98–107 (2018).

[10] **Li X, Liu B, Yu G, Dai, W., Hu, J., Luo, E. and Li, H.** Experimental validation and numeric optimization of a resonance tube-coupled duplex Stirling cooler. Applied Energy, 207:604–12 (2017).

[11] **Chen, H., and Longtin, J.P.,** Performance analysis of a free-piston Vuilleumier heat pump with dwell-based motion. Applied Thermal Engineering, 140:553–63 (2018).

[12] **Wong, H. M., and S. Y. Goh**. Experimental comparison of sinusoidal motion and non-sinusoidal motion of rise-dwell-fall-dwell in a Stirling engine. Journal of Mechanical Engineering and Sciences 14, (3): 6971-6981 (2020).

[13] **Li RJ, Grosu L, Queiros-Condé D.** Losses effect on the performance of a Gamma type Stirling engine, Energy Conversion Management, 114:28–37 (2016).

[14] **Liao C, Jiang T, Hofbauer P, Ye W, Liu J, Luo B, and Huang Y.** Simplified model and analysis for the performance of Hofbauer-Vuilleumier heat pump. International Journal of Refrigeration. 1 (103) 126-34 (2019).

[15] **Shang, S., Li, X., Wu, W., Wang, B. and Shi, W.**, Energy-saving analysis of a hybrid power-driven heat pump system. Applied Thermal Engineering, 123, pp.1050-1059 (2017).

[16] **Dogkas, G. and Rogdakis, E.,** A review on Vuilleumier machines. Thermal Science and Engineering Progress, 8: 340-354 (2018).

[17] **Hèyihin, A.G., Awanto, C., Anjorin, M. and Lanzetta, F.,** Thermodynamic analysis of the Stirling Duplex machine. In Advanced Engineering Forum. 30:. 80-91. Trans Tech Publications Ltd (2018).

[18] **Guo, T., Jiang, T., Zou, P., Luo, B., Hofbauer, P., Liu, J. and Huang, Y.,** Analytical model for Vuilleumier cycle. International Journal of Refrigeration, 113:126-135. (2020).

[19] **Ranieri, S., Prado, G.A. and MacDonald, B.D**., Efficiency reduction in Stirling engines resulting from sinusoidal motion. Energies, 11(11), p.2887. (2018).

https://doi.org/10.3390/en11112887

[20] **Červenka L.,** Idealization of the real Stirling cycle, MECCA Journal of Middle European construction and design of cars, Vol. 14 No. 03 (2016).

[21] **Briggs M. H.** Improving power density of free-piston Stirling engines, 14th International Energy Conversion Engineering Conference, July 25-27, Salt Lake City, Utah USA, (2016), https://doi.org/10.2514/6.2016-5016.

[22] **Gopal, V.K**, "Active Stirling Engine ", PhD Theses University of Canterbury. Electrical and Computer Engineering, New Zealand.

[23] **Craun M., Bamieh, B**. Control-Oriented Modeling of the Dynamics of Stirling Engine Regenerators, Journal of dynamic systems, measurement, and control, ASME Transactions, 140(4): 041001, Paper No: DS-15-1652 (2018) https://doi.org/10.1115/1.4037838

[24] **Masser, R.; Khodja, A**.; Scheunert, M.; Schwalbe, K.; Fischer, A.; Paul, R.; Hoffmann, K.H. Optimized Piston Motion for an Alpha-Type Stirling Engine. Entropy, 22, 700 (2020).

[25] **Podešva J, Poruba Z.** "The Stirling engine mechanism optimization." Perspectives in Science. 1 (7):341-6, (2016).

[26] **Scheunert, M., Masser, R., Khodja, A., Paul, R., Schwalbe, K., Fischer, A. and Hoffmann, K.H**., Power-optimized sinusoidal piston motion and its performance gain for an Alpha-type Stirling engine with limited regeneration. Energies, 13(17), p.4564. (2020) doi:10.3390/en13174564

[27] **Gussoli M.K., de Oliveira JC, Higa M.** Investigation on volume variation for alpha Stirling engines on isothermal model. Revista de Engenharia Térmica. 19 (2):10-6 (2020).

[28] **Nicol-Seto, M. and Nobes, D**., Experimental evaluation of piston motion modification to improve the thermodynamic power output of a low temperature gamma Stirling engine, E3S Web of Conferences 313, 04002, 19th International Stirling Engine Conference, (2021)

تأثيرات حركة المكبس على الطاقة الناتجة من آلات دورة ستيرلينغ

ماجد معلا الحازمي

الهندسة الميكانيكية، جامعة الملك عبد العزيز

جدة، المملكة العربية السعودية

مستخلص. تستخدم هذه الورقة نموذجًا بسيطًا لتقدير الطاقة المنتجة من محرك ستيرلينغ عند إعطاء المكابس حركة مستمرة بنمط محدد وتردد ثابت وانزياح طور متغير لنسب درجة حرارة تشغيلية مختلفة. تم فحص نمطين للحركة المستمرة ، الجيبية والجيبية المعدلة ، ضد الحركة المتقطعة للدورة المثالية. الطاقة الناتجة من المحركات ذات المكابس المتحركة باستمرار أقل من الطاقة الناتجة من الدورة المثالية. تنخفض نسبة الطاقة مع زيادة نسبة درجة الحرارة. أعلى طاقة منتجة بنسبة درجة حرارة ١.٥ ، هي ٩٧٪ من الدورة المثالية وتحدث عند تحول طور قدره ٨١ درجة. يعمل التشغيل عند ±١٠ درجة من أعلى حالة تغيير طور الطاقة على تقليل طاقة المنتجة بنسبة ٥-٧٪. بالنسبة للحركة الجيبية المعدلة ، تكون أعلى طاقة منتجة ٨٨٪ عندما يكون تغيير الطور ٥٥ درجة. يعمل التشغيل عند رجات من أقصى حالة تغيير طور الطاقة على تقليل طاقة المنتجة بنسبة ٢٪. علاوة على ذلك ، عند فرق الطور المتسبب في أعلى طاقة منتجة، تنخفض نسبة الطاقة من ٩٧٪ إلى ٩٣٪ ، للحركة الجيبية حيث تتغير نسبة درجة حرارة الدورة من ١.٥ إلى ٣. أما بالنسبة للحركة الجيبية المعدلة فإن الطاقة المنتجة تنخفض من ٨٨٪ إلى ٧٨ ٪ من قيمتها العليا.